International Journal of Mining Science and Technology 33 (2023) 73–81

Contents lists available at ScienceDirect

International Journal of Mining Science and Technology

journal homepage: www.elsevier.com/locate/ijmst

Methodology for the estimation of expansive cement borehole pressure

Kelly-Meriam Habib *, Isaac Vennes, Hani S. Mitri

Department of Mining and Materials Engineering, McGill University, Montreal H3A 0E8, Canada

ARTICLE INFO

Article history:
Received 9 January 2022
Received in revised form 13 September 2022
Accepted 27 September 2022
Available online 14 December 2022

Keywords:
Rock fragmentation
Soundless chemical demolition agents
Expansive cement

ABSTRACT

This work is part of a multi-phase project which aims to develop a sound methodology for rock fragmentation in underground mines using expansive cement. More specifically, it is the first phase of the project which focuses on laboratory tests to investigate the mechanical performance of expansive cement, also known as soundless chemical demolition agents (SCDA). This paper reports the results of laboratory tests conducted on instrumented thick-walled cylinders filled with expansive cement. Expansive pressure evolution and temperature variation with time are first examined for different borehole diameters. The classical analytical method for expansive pressure estimation is validated with direct pressure measurement using high-capacity pressure sensor, and an empirical model is obtained. A new methodology based on iterative procedure is developed using axisymmetric finite element modelling and test results to derive the modulus of elasticity of the expansive cement at peak pressure. The results of this study show that the expansive pressure increases with borehole diameter when the rigidity of the steel cylinder is constant reaching 83 MPa for a 38.1 mm borehole. It is also shown that the expansive pressure decreases significantly with increased cylinder rigidity for the same borehole diameter. The newly developed methodology revealed that the modulus of elasticity of expansive cement at peak pressure is estimated at 8.2 GPa. A discussion on the extension of the findings of this work to hard rock mining applications is presented.

1. Introduction

Class G cement, a common type of commercially available SCDA, is mainly composed of lime or calcium oxide which expands during curing when in confined conditions such as in a borehole. The source of expansion is owed to the hydration reaction of lime which results in the generation of portlandite crystals ($Ca(OH)_2$ or calcium hydroxide) as shown in Eq. (1) [1].

$$CaO + H_2O \rightarrow Ca(OH)_2 + 15.2\,\text{kcal/mol} \quad (1)$$

Fig. 1 is a schematic presentation of the expansion mechanism for lime based expansive cement. As shown in Fig. 1a expansion starts off with the hydration of CaO resulting in the growth of solid calcium hydroxide crystals which come into contact with each other at a point, known as the critical degree of hydration (Fig. 1b). Beyond the critical degree of hydration (Fig. 1c) [2,3], further growth of calcium hydroxide crystals results in the generation of expansive pressure under restrained condition.

Expansive cement can be used as a method for rock or concrete fragmentation by means of injecting the mixture into drilled holes in the material of interest. Within a confined hole, pressure develops over time causing circumferential or tangential tensile stress. As shown in Fig. 2, a fracture is created at the weakest section along the inside surface of hole. This occurs at a point where this surface intersects the free surface which is the hole boundary. The initial crack generation will only propagate when the tensile stress exceeds the tensile strength of the rock. Therefore, the tangential tensile stress generated by the SCDA or expansive cement, is responsible for fracturing of rock. Currently, this method is used commonly in surface applications such as the demolition of concrete foundations in rehabilitation projects and fragmentation of rock in dimension stone quarries [4,5].

The early literature on expansive cement generally focuses on the investigation of the factors that affect the performance of expansive cement such as ambient temperature, borehole spacing and block pattern, water content etc. [1,6,7,8,9]. The research is now directed at the implementation of expansive cement in the field. To do so, finite element modeling has been used by Cho et al. to predict the minimum pressure required of the SCDA for concrete demolition, hole spacing, and material properties [10]. Others used expansive cement to investigate discontinuity persistence along incipient discontinuities in the rock mass [11]. Expansive cements have also been used for well cementing as well as stimulating and enhancing fracturing for the oil and gas industry [12,13]. More recent work involved experimental work on dynamic

* Corresponding author.
E-mail address: kelly-meriam.habib@mail.mcgill.ca (K.-M. Habib).

https://doi.org/10.1016/j.ijmst.2022.09.019
2095-2686/

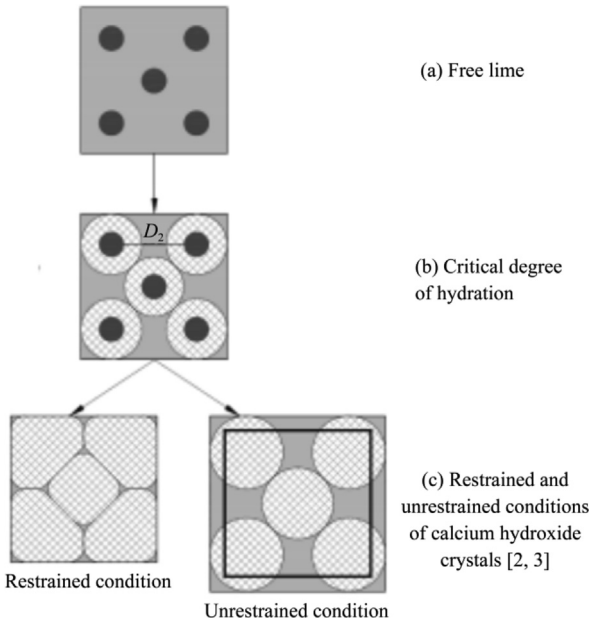

Fig. 1. Sphere model for expansive pressure of calcium hydroxide.

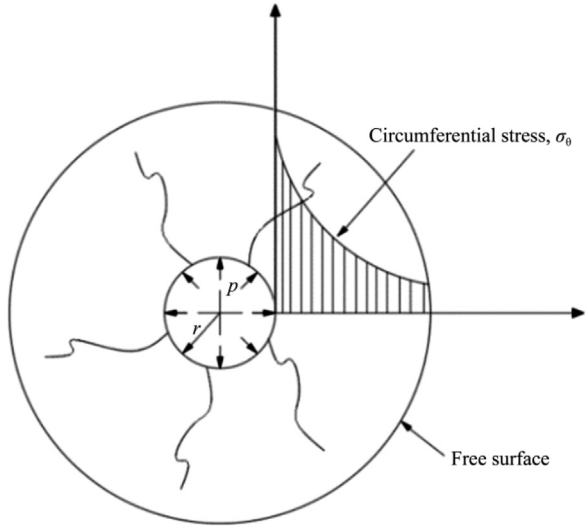

Fig. 2. Fractural propagation in a borehole (modified after [4]).

propagation of fractures under various biaxial conditions where expansive cement is injected in two holes [14]. While much work has been dedicated to numerical simulation, researchers in Iran have suggested an algorithm to evaluate the first crack length with the use of expansive cement and verified it in a granite quarry in Iran [15]. More large-scale testing have been conducted by Tang et al. whereby expansive cement was used to weaken the strong roof at the Pingdingshan coal mine to prevent rock bursts [16]. Zhang et al. used expansive cement or directional roof cutting at the Donglin coal mine [17]. Others focused on the handling of SCDA by developing special self-swelling SCDA cartridges to be used in up-tilt boreholes [18].

In this paper, the main research focus is proper quantification of expansive cement pressure and the role of host medium condition—an aspect that has often been overlooked by previous research. As shown in Table 1, manufacturers of different commercially available SCDA do report expansive pressures that range from 80 to 137 MPa in temperatures between −8 to 40 ℃ [19–24]. However, how the expansive pressure is measured is unclear. The quantification of expansive cement pressure has been studied by many researchers in literature to explore potential applications that require a minimum pressure.

Table 1
Reported expansive pressure of different commercially available expansive cement [19–24].

Commercially available SCDA	Recommended temperature (℃)	Maximum pressure (MPa)
Betonamit	−5 to 35	80
Bristar	−5 to 35	30
Dexpan	−5 to 40	124
Expando	0 to 35	124
Ecobust	−8 to 35	137

The thick-walled cylinder method is used by many researchers to quantify the expansive pressure of commercially available expansive cement, such as Bristar, Dexpan, and Betonamit. The expansive pressure can be calculated by pouring the expansive agent in a hollow thick-walled cylinder, whereby the cylinder is considered thick-walled when the thickness $t \geq 0.1$ the inner cylinder radius r_i (known as Hertzberg criterion). One or more strain gauges are installed on the outer surface of the cylinder in the tangential direction at about mid-height of the cylinder. The tangential strains of the specimen are then used to calculate the circumferential or radial pressure generated by the expansive agent as shown in Eq. (2) [24].

$$p_i = \frac{E\varepsilon_\theta\left(r_o^2 - {r_i}^2\right)}{2r_i^2} \tag{2}$$

where p_i is the internal pressure, which in this case is the expansive pressure, MPa; E the modulus of elasticity of the steel cylinder (200000 MPa); r_o the outer radius of cylinder, mm; r_i the inner radius of cylinder, mm; and ε_θ the circumferential or tangential strain on the external surface of the test cylinder.

Natanzi et al. [6] investigated the effect of ambient temperature on the pressure development in two commercial expansive cement brands: Bristar and Dexpan. Using a 170 mm long, thick-walled cylinder (r_o=21 mm, r_i=18 mm) Dexpan exhibited a maximum expansive pressure of 28 and 8 MPa at ambient temperature of 19 and 2 ℃, respectively while Bristar exhibited an expansive pressure of 65 and 18.5 MPa at the same ambient temperatures, respectively [6]. A recent study by Laefar et al. [25] has also conducted tests using thick-walled cylinders submerged in cold water baths to provide a heat sink to the surrounding rock or concrete. Their experimental results show that quadrupling the volume of SCDA and keeping the water bath temperature constant resulted in expansive pressure increase of 700%. Soeda [26] conducted studies on developing their own SCDA in granular form versus commercialized SCDA that is in its powder form to provide more space between grains for steam release and prevention of the gun phenomenon where the expansive cement spews out of the borehole. Using the thick-walled cylinder configuration, 19.6 MPa was achieved in 18 h with the commercialized SCDA while their own developed SCDA, Type 1 and Type 2 generated 29.4 MPa in 2 h and 29.4 MPa in 3 h, respectively [26]. Studies conducted by Gholinejad and Arshadnejad [27] tested the pressure in thick-walled cylinders made from different materials namely steel, aluminum, concrete, and high strength plastic. Steel (E=205 GPa, r_i=10 mm, r_o=20 mm) generated 34 MPa in 30 h; aluminum (E=71 GPa, r_i=20 mm, r_o=30.25 mm) generated 30 MPa; concrete (E=12.1 GPa, r_i=18 mm, r_o=41 mm) generated 16–17 MPa and high strength plastic (r_i=7.5 mm, r_o=12.5 mm) generated 0–1 MPa [27]. Other studies conducted by Hanif [5] studied the effect of variable hole spacing in granite using Bristar-100S for optimal fracturing.

Preliminary work involved the quantification of expansive pressure where 52 MPa was achieved in 144 h using thick-walled cylinder where both ends were constrained by 18 mm thick steel plates [5]. Dowding and Labuz [28] have also used the thick-walled cylinder configuration to quantify the pressure of Bristar and selected the dimensions of the steel cylinder by equating the rigidity of the steel cylinder, R, to that of the rock as shown in Eq. (3).

$$R = \frac{E\left(r_o^2 - r_i^2\right)}{r_i^2} \tag{3}$$

It was shown that steel cylinders with approximately equal rigidities, but different geometries result in the same expansive pressure [28].

A modification of the thick-walled cylinder method termed the upper end surface method (UESM) was recently developed to estimate the pressure of SCDA. A notable difference between the thick-walled cylinder method and UESM is that the UESM container is composed of 7075 aluminum alloy rather than steel, which offers a longer path of heat transfer as well as a higher material heat conductivity, thereby avoiding lower temperature to the affixed strain gauge. Their studies confirm that both the thick-walled cylinder configuration and their newly developed UESM generate consistent results with each other [29].

The differences in expansive pressure estimates may be attributed to variations in the experimental configuration (in this case geometry) as well as the brand of expansive cement being used. Many researchers lack explanation behind the selection of the steel geometry which may differ in rigidities thereby may not reflect an accurate representation of SCDA pressure in hard rock. Since many factors must be taken into consideration when quantifying expansive cement pressure, no singular expansive pressure is reported for any expansive cement product. It is noteworthy that due to the simplicity of Eq. (2), much of the previous studies rely on its use for borehole pressure estimation. A direct measurement of expansive pressure would be important not only to validate Eq. (2) but also to reveal the actual expansive cement pressure by deriving a correction factor to the analytical model (Eq. (2)). A more robust approach in quantifying pressure is therefore required to properly estimate the obtained pressures in rock.

As shown in Eq. (1), the hydration reaction is an exothermic reaction which can sustain the expansive cement and host medium above ambient temperature. The relatively high temperature increases the rate of hydration of lime, one of the main sources of expansion development [7]. Given the temperature of the expansive cement is also dependant on the thermal properties of the host medium, such as the heat capacity, heat conductivity, and density, the rate of reaction and therefore the rate of pressure generation is related to the thermal properties of the host medium. In addition, it is unclear if the rate of SCDA expansion affects the ultimate pressure given all other parameters are kept constant. It is therefore ideal to replicate the thermal properties of rock with the steel cylinder experiment, which is why past studies have tended to use thicker steel cylinders which provide a larger heat sink equivalent to an infinite rock medium [1,5,6,27,28]. However, given steel has a higher modulus of elasticity than rock, a balancing act between rigidity and heat sink size is required.

It is also postulated that larger SCDA borehole size increases the rate of reaction as the heat generating mass of SCDA increases proportionally to the cube of the radius, while the borehole surface over which heat dissipates increases proportional to the square of the radius [7]. The effect of borehole size is therefore investigated while keeping the host medium rigidity constant. The effect of host medium radial rigidity is also investigated while keeping the borehole size constant. Overall, sufficient wall thickness is selected to fit the thick-walled criterion while selecting sufficient wall thickness to dissipate heat. The goal of this study is to rationalize a systematic methodology to assess the pressure generation in varying host conditions to understand expansive cement performance in different host materials such as hard rock. Also, a simple iterative methodology is proposed for the estimation of the SCDA modulus of elasticity at peak pressure using direct pressure measurement and numerical modeling.

2. Materials and method

2.1. Setup

Commercially available expansive cement selected for this investigation is Betonamit. The expansive cement was mixed with a water to cement ratio of 0.2 with a water temperature of 20 ℃. A water-to-cement ratio of 0.2 was adopted as per the manufacturer's instructions. Other ratios up to 0.3 were tried but did not produce optimal results. To ensure reliability and repeatability, all slurries were poured immediately upon mixing into a thick-walled steel cylinder. The expansive cement was poured by gravity into the borehole as per the instructions of the manufacturer. No sealing was deemed necessary. The expansive pressure was measured by using temperature compensating strain gauge glued to the outer surface of steel at mid-height. All tests were conducted at room temperature of 21–22 ℃. The tangential strain was recorded over a period of 24 h using the Micro-Measurements System 8000 Data Acquisition System. The expansive pressure is estimated using Eq. (2) with modulus of elasticity of the steel material E=200 GPa. It is to be noted that while the rock mass is generally heterogeneous, the rock material surrounding an SCDA hole is considered intact. Clearly, the presence of joints in the rock mass would help accelerate the fracturing process. The assumption of using intact material as a host medium is reasonable considering the scale of the problem. Most research on borehole mechanics considers intact rock material being stronger than the jointed rock mass, e.g., drilling and blasting [30–33]. Thus, the use of steel material as a host medium is deemed suitable. The rigidity of the steel for each test is also estimated using Eq. (3).

As Eq. (2) [24] used to calculate the expansive cement radial pressure is based on the assumption of infinitely long pipe without a base, it deemed important to verify the minimum required length of the thick-walled cylinder to justify its use for pressure calculation. To validate the selected length of the cylinder and mid-height position of the strain gauge, several finite element (FE) axisymmetric Abaqus models were built: the first has an aspect ratio of 4 with a base plate as per the experiment while other FE models employed longer and shorter cylinders with a base plate, and aspect ratios larger and smaller than 4. Comparison of mid-height tangential strain of all FE models showed that the tangential strain readings are not influenced by the base plate when the aspect ratio is 4 or more. The tangential strain is nearly uniform along the length of the outer surface of the cylinder except near the base plate. Therefore, an aspect ratio of 4 (which is also the minimum recommendation by the manufacturer) is adopted for this study. FE modelling is discussed in Section 3.4.

The experiment is designed to investigate the use of expansive cement for drift development in hard rock mines, with a hypothetical drift development cycle of 6 h. Therefore, equal importance is given to the ultimate pressure as well as the pressure in 6 h.

2.2. Test identification

To identify different tests, the following nomenclature M-S-ID-OD-TB-XX was used. Refer to Table 2 for abbreviations.

Table 2
Abbreviations for test identification.

Abbreviations	Test identification
M	Material e.g., S for steel
S	Shape of host medium, e.g., C for Cylinder
ID	Internal diameter in inches, e.g.,125 for 1.25"
OD	Outer diameter in inches, e.g., 175 for 1.75"
TB	Type of base e.g., S for solid, W for welded
XX	Serial number

The cylinder length L, was fixed at 4 times the inner diameter as discussed above. Refer to Fig. 3a and b for steel configuration geometries.

2.3. Tested configurations

Table 3 lists the three steel cylinder configurations that were tested in this study. As can be seen, the borehole sizes of 25.4 mm (1"), 31.75 mm (1.25") and 38.1 mm (1.5") are investigated in this study. To ensure that the influence of the borehole size is adequately examined, the cylinders were fabricated to produce the same host medium rigidity as defined in Eq. (3).

3. Experimental results and discussion

3.1. Effect of borehole size

As shown in Table 3, three borehole sizes of 25.4 mm (1"), 31.75 mm (1.25") and 38.1 mm (1.5") are investigated while keeping the steel cylinder rigidity nearly constant as calculated from Eq. (3). Specimens S–C–100–175-W, S–C–125-227-S, and S–C–150-275-S have rigidities of 412500, 460628 and 472222 MPa respectively. Duplicates for each test were done to ensure repeatability and reliability. The 25.4 mm (1") borehole is used as reference to assess the effect of expansion pressure with increasing borehole size. A clear trend is observed with specimens of varying borehole

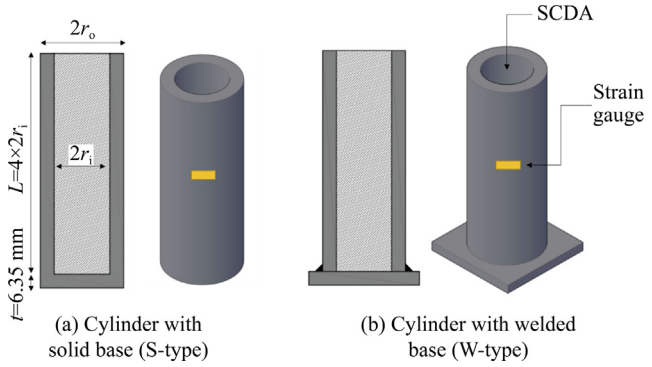

Fig. 3. Steel cylinder configurations tested in this research.

Table 3
Summary of tested steel cylinder configurations.

Sample configuration	Inner diameter r_i (mm)	Outer diameter r_o (mm)	Rigidity (MPa) Eq. (3)
S–C–100-175-W	25.4 (1")	44.45 (1.75")	412500
S–C–125-227-S	31.75 (1.25")	57.60 (2.27")	460628
S–C–125-210-S		53.34 (2.1")	365384
S–C–150-275-S	38.1 (1.5")	69.85 (2.75")	472222
S–C–150-340-S		86.36 (3.40")	1008889
S–C–150-420-S		106.68 (4.20")	13680000

size and similar rigidities as shown in Fig. 4 whereby the development expansive pressure over time is proportional to the borehole size. The 38.1 mm (1.5") borehole exhibits a maximum pressure up of 60 MPa in only 6 h and the 31.75 mm (1.25") borehole shows a lower pressure 39.2 MPa in 6 h. However, a similar average maximum pressure is achieved for both 31.75 mm (1.25") and 38.1 mm (1.5") borehole size with pressure of 55.4 and 60 MPa respectively. Specimen S–C–100-175-W exhibits a lower pressure of 16.9 and 43 MPa in 6 and 24 h respectively.

3.2. Effect of host medium rigidity

The effect of host medium rigidity was tested while keeping the borehole size constant at 38.1 mm (1.5"). As shown in Table 3, three geometries were tested to investigate low to high rigidity host mediums calculated by Eq. (3) (low rigidity: S–C–150-275-S, medium rigidity: S–C–340-S, high rigidity: S–C–150-420-S). The experimental results are shown in Fig. 5. As can be seen, a high host rigidity of 13680000 MPa (S–C–150-420-S) generates significantly less pressure than a low rigidity host of 472222 MPa (S–C–150-275-S) at 24 h which generated expansive pressures of 29.7 and 60 MPa respectively while a medium host rigidity of 1008889 MPa (S–C–150-340-S) generated pressures of 43.6 MPa.

The expansive pressure increases by 98.1% with a low rigidity compared to a high rigidity in 6 h. It is also shown that the low rigidity host reaches its maximum expansive pressure early on in just 6 h with 60 MPa. This increase in reaction rate can once again be attributed to an increase in expansive cement temperature. Since the specimens with a lower thickness provide a smaller heat sink for the expansive cement, the expansive cement temperature and therefore reaction rate is expected to be higher. However, it is also observed that the ultimate expansive cement pressure is also higher. It is once again unknown if the reaction rate and ultimate pressure are directly linked. Nonetheless, the experimental results show that the borehole size is not the only parameter affecting ultimate pressure, as tested in Section 3.1. It is observed that increasing the rigidity of the host medium to SCDA expansion may inhibit the reaction, reducing the ultimate pressure after 24 h. In any case, it can be seen that ultimate pressures obtained in steel will differ from those obtained in rock, caused by either differing host rigidity, heat capacity, density, and heat transfer rate.

To conclude, the steel cylinder experiment is a well-established reference method that is commonly used to estimate the expansive cement peak pressure [7,24]. This test is adopted because the mechanical properties of the steel material are known, and the tensile strength is high enough to sustain the expansive pressure to its peak value. In practical rock fragmentation applications, it is reasonable to assume that $r_o \gg r_i$, hence the rigidity from Eq. (3) is reduced to:

$$R = E\left(\frac{r_o}{r_i}\right)^2 \tag{4}$$

The above equation suggests that larger SCDA hole diameter would reduce the host medium rigidity. The trends observed in the steel cylinder experiment can then be extrapolated to practical applications. However, these will be subject to further validation, which is beyond the scope of this work.

3.3. Direct pressure measurement

The thick-walled cylinder experiment for the expansive cement pressure calculation has the advantage of being simple and economical as it only requires the use of a strain gauge mounted on the outer surface of the cylinder. However, it has never been validated with direct measurement of the actual internal pressure in

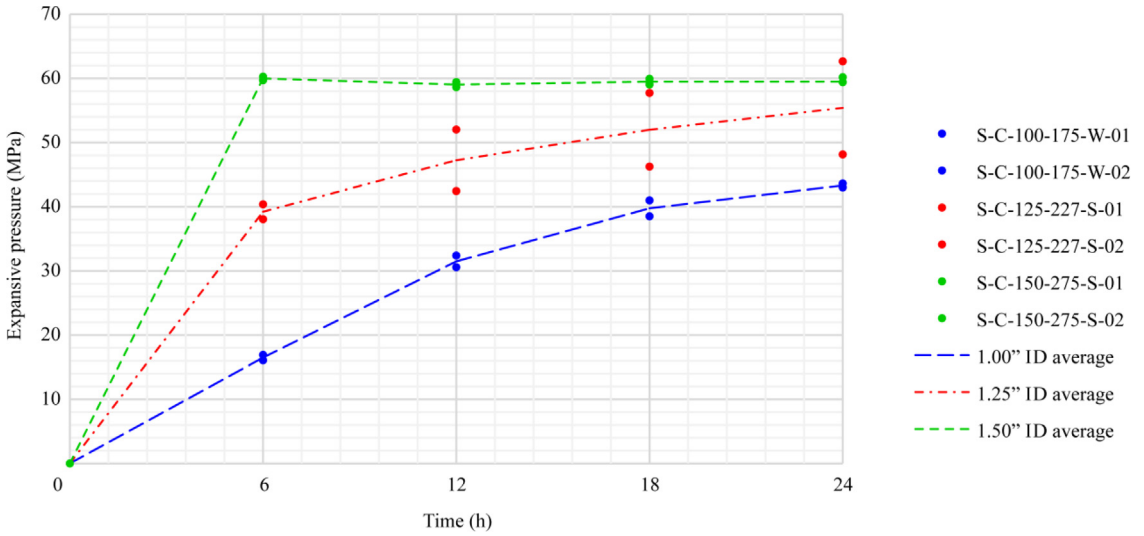

Fig. 4. Expansive pressure of expansive cement with varying borehole size and constant rigidity (*R*).

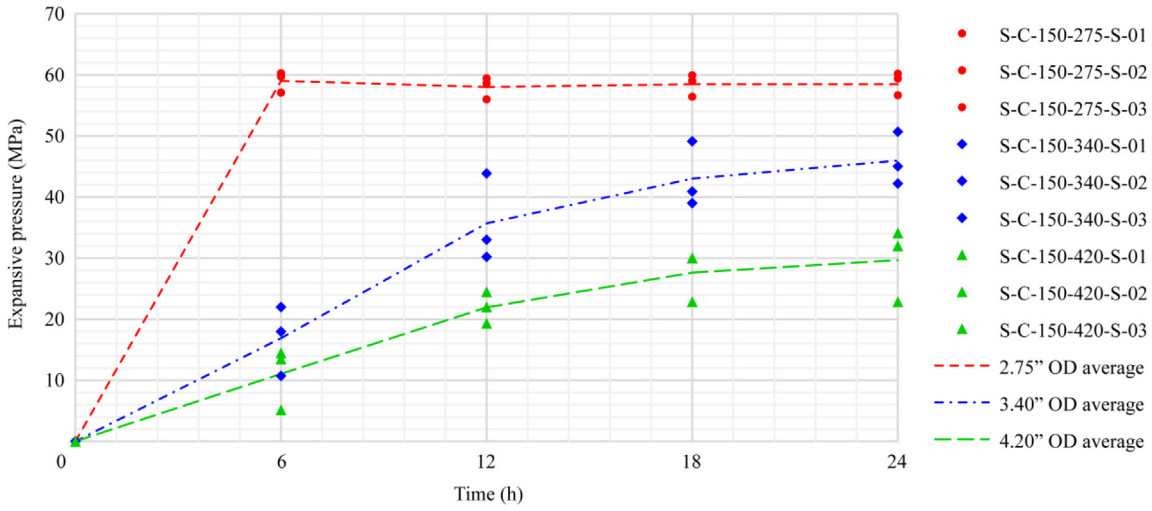

Fig. 5. Expansive pressure evolution for varying host medium rigidity and a constant borehole size 38.1 mm (1.5").

the cylinder. It is therefore important however to verify the accuracy of the method. To do so, a second experiment was designed and implemented with a pressure sensor inserted through the cylinder wall at its mid-height as shown in Fig. 10a and c along with a strain gauge on the outer surface. The sensor is model XPM6-1KBG and can measure a pressure range from 20 to 2000 bars. It would directly measure the actual pressure, P_a, which can then be compared to the calculated pressure P_c obtained from the strain gauge reading and Eq. (2).

The pressure sensor was directly connected to DAQ measuring the SCDA expansive pressure over a period of 24 h. A series of 6 direct pressure measurement tests was conducted with 2 tests for each SCDA hole size namely 25.4 mm (1.00"), 31.75 mm (1.25"), and 38.1 mm (1.5"). The pressure evolution and temperature readings with time is depicted in Figs. 7 and 8 respectively.

As shown in Fig. 7, pressures of 8, 55 and 65 MPa are achieved in 6 h for specimen S–C–100-175-W, S–C–125-210-S and S–C–150-275-S respectively (Refer to Table 3 for specimen specifications). It is also shown that pressures of 56 , 71 and 83 MPa are achieved in 24 h for specimen S–C–100-175-W, S–C–125-210-S and S–C–150-275-S respectively (Refer to Table 3 for specimen specifications). The measured pressure data is also in accordance with the results presented in Section 3.1, where a higher ultimate pressure is attained faster for larger borehole diameters.

As shown in Fig. 6c, the heat of hydration produced during the SCDA reaction was also measured throughout the testing period using thermocouples embedded in the SCDA. As shown in Fig. 8, a peak hydration heat of 50.8 ℃ was recorded at 5 h for specimen ID S–C–150-275-S while a peak hydration of 39.9 and 40.1 ℃ was recorded at 5 h for specimen ID S–C–100-175-W and S–C–150-275-S. Fig. 8 shows that the borehole size is correlated to the degree of heat generation. Based on the experimental results, higher heat generation corresponds to higher SCDA expansive pressure, which is owed to the increased mass of SCDA relative to the surface area on which pressure is applied and through which heat is exchanged with the host medium. This is in accordance with studies conducted by Hinze and Brown, [7] which elucidate that a large diameter provides more space for free lime to be hydrated in the borehole. As shown in Eq. (1), the hydration reaction is an exothermic one where this heat indirectly speeds the rate of pressure evolution [7].

Fig. 9 Plots the comparison between the actual and calculated peak pressure after 24 h. As can be seen, the actual peak pressure is consistently higher.

(a) Side view of XPM6-1KBG miniature pressure sensor

(b) Top view of XPM6-1KBG miniature pressure sensor threaded into wall cylinder

(c) Expansive cement filled cylinder with embedded temperature sensor

Fig. 6. Direct pressure measurement in specimen S–C–150-275-S.

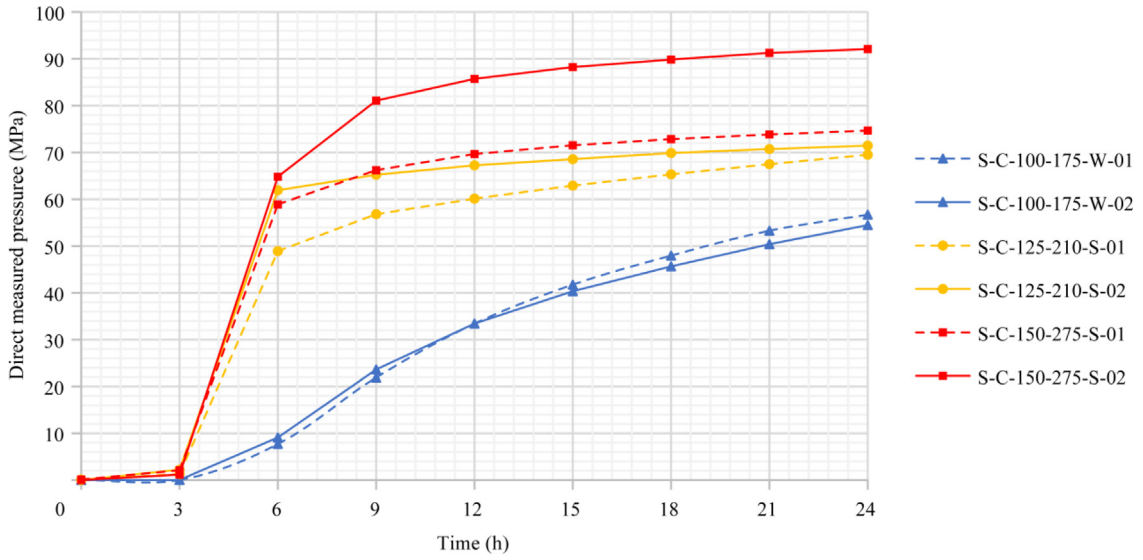

Fig. 7. Measured expansive pressure of varying borehole size.

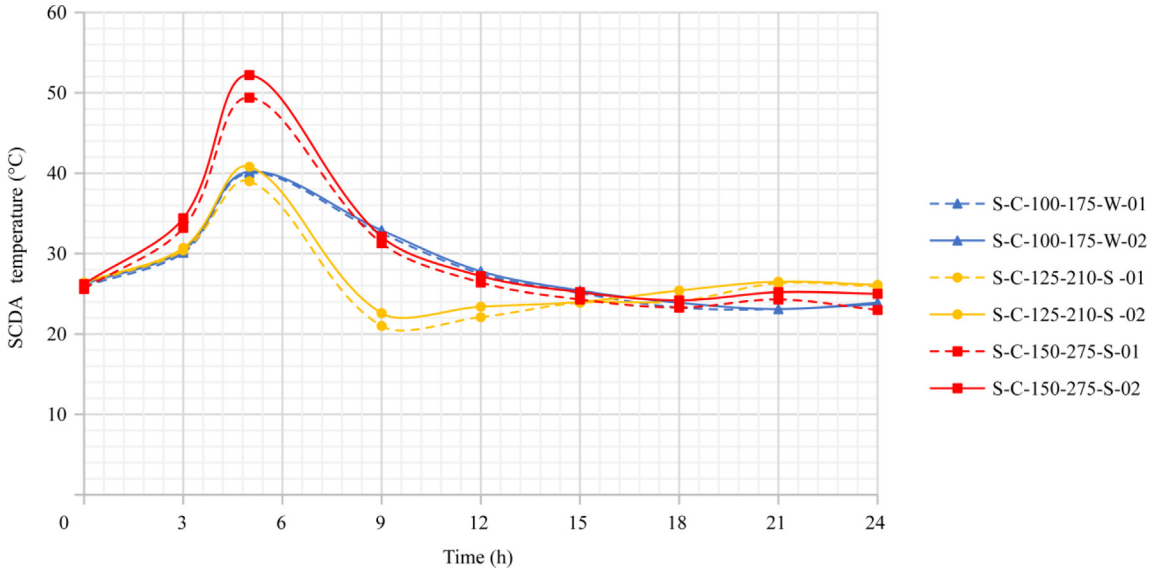

Fig. 8. Expansive cement heat of hydration with time of varying borehole size.

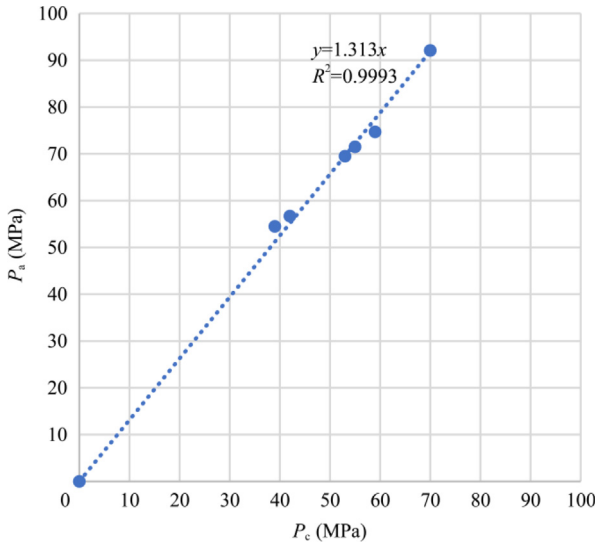

Fig. 9. Measured peak pressure (P_a) vs calculated peak pressure (P_c).

A best fit line with an R^2 factor of 0.999 is obtained as follows,

$$P_a = \alpha P_c \quad (5)$$

where α=1.31 is a correction factor to the calculated pressure. Although costly, the direct pressure measurement experiment confirms the validity of the less expensive method employing only a strain gauge on the outer surface, albeit with a correction factor α.

Table 4
Material properties for the FE model.

Material	Young's modulus (GPa)	Poisson's ratio
SCDA	TBD	0.2
Steel	200	0.3

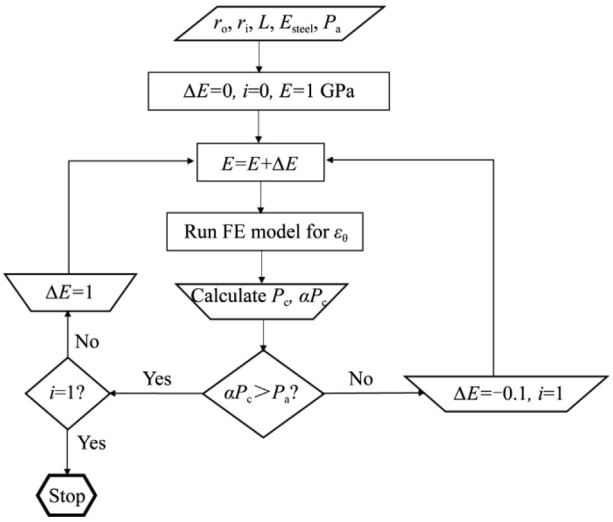

Fig. 11. Iterative procedure to determine SCDA modulus of elasticity of expansive cement at peak pressure.

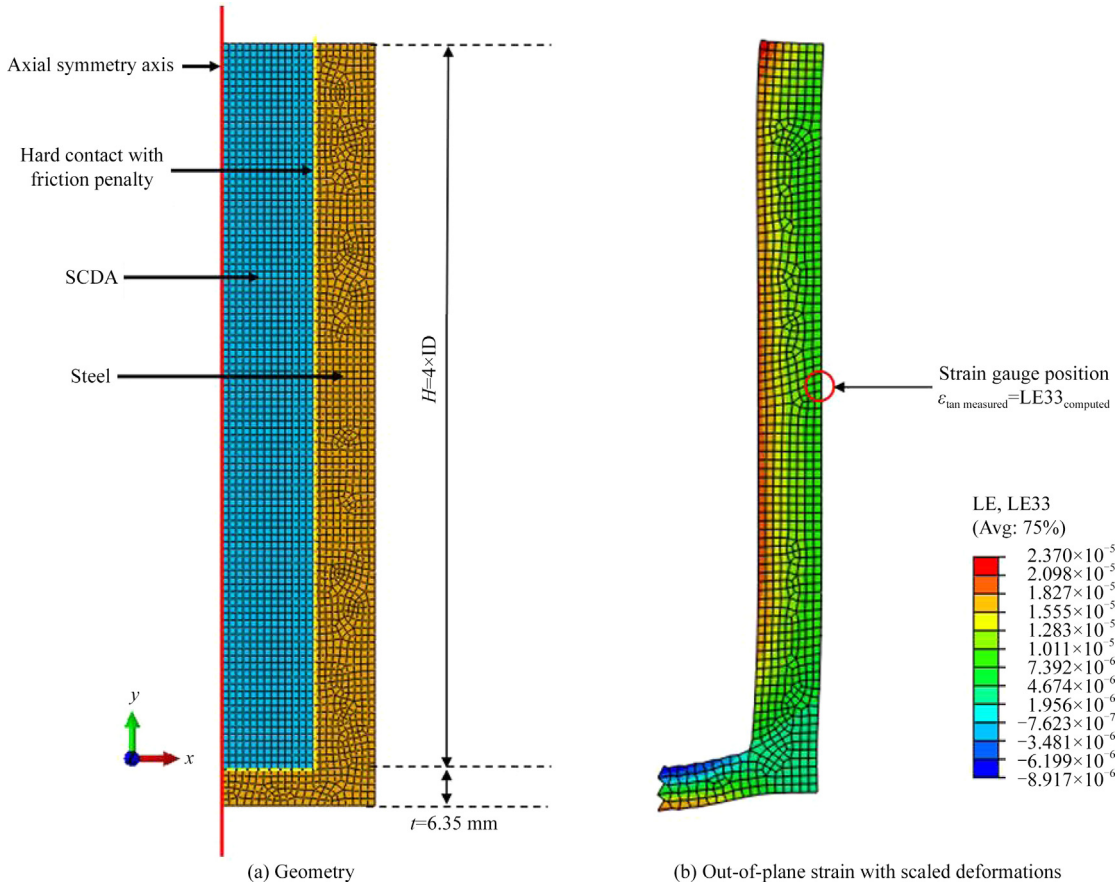

(a) Geometry (b) Out-of-plane strain with scaled deformations

Fig. 10. Model of axisymmetric steel cylinder.

Table 5
Modulus of elasticity of expansive cement with varying borehole size.

Specimen	100-175-01	100-175-02	125-210-01	125-210-02	150-275-01	150-275-02
E_{Peak} (GPa)	8.1	8.1	8.2	8.2	8.3	8.35

3.4. Finite element model

Numerical modelling studies of expansive cement mechanical behaviour could benefit from the knowledge of the peak modulus of elasticity of the expansive cement at peak pressure, E_p. As the actual pressure value is known from the direct pressure measurement experiment, it is used as a model input parameter to obtain the modulus of elasticity of the expansive cement material using the axisymmetric model through simple iterative process.

First, an axisymmetric finite element (FE) model of the steel cylinder was constructed in Abaqus/CAE 2019. The purpose of the model is to derive the elasticity of the expansive cement material for a given expansive pressure as will be explained further. As shown in Fig. 10, the FE model is axisymmetric and linear elastic; it consists of two zones: A steel cylinder part and an expansive cement part. The contact surface between the steel and SCDA is treated as hard contact in the normal direction and frictional in the tangential direction with a friction penalty of 0.3. Table 4 presents the material properties. The Poisson's ratio of the SCDA is assumed to be 0.2 and the modulus of elasticity is to be determined (TBD).

The SCDA pressure is modeled as initial stress or pre-defined field in the initial step. The pressure is subsequently released in a second static step. From the model output, the tangential strain component LE33 at the location of the strain gauge (Fig. 10b) is extracted.

As shown from the flowchart in Fig. 11, the iteration begins with an initial value of E=1 GPa and subsequent increments ΔE=1 GPa. For a given steel cylinder specimen (r_o, r_i, L, E_{steel}), the FE model is run for the tangential strain ε_θ from which the corrected pressure αp_c can be calculated from Eq. (5). Iteration continues with ΔE=1 GPa and subsequently with ΔE=−0.1 GPa until the measured and calculated pressures match. The calculation process was done for all six specimens tested with the pressure sensor.

The results shown in Table 5 reveal that E_p varies between 8.1 and 8.35 GPa with an average of 8.2 and a coefficient of variation of only 0.01243. This SCDA peak modulus of elasticity can be used as an input parameter for future modelling studies on expansive cement.

4. Conclusions

This work is part of a multi-phase project which aims to develop a sound methodology for rock fragmentation in underground mines. More specifically, it is the first phase of the project which focuses on laboratory tests to investigate and optimize the mechanical performance of SCDA in various conditions. Based on the findings of this work, future work will extend to the investigation of SCDA performance in hard rocks commonly encountered in Canadian mines such as granite, gabbro, and norite. This paper examines expansive cement pressure variation with host medium rigidity—an aspect that has often been overlooked by previous research. The effect of borehole size with time is first investigated while keeping the host medium rigidity constant for borehole sizes of 25.4 mm (1"), 31.75 mm (1.25"), and 31.8 mm (1.5"). The results show that the estimated peak expansive pressure is proportional with the borehole diameter. This is in line with previous research findings [1,7]. However, when the host medium rigidity is increased, the estimated expansive pressure is reduced significantly. The practical implication of this finding is that the expansive SCDA peak pressure in hard rocks such as gabbro and norite commonly encountered in metal mines is likely to be less than that in sedimentary rocks such as limestone and mudstone commonly found in coal mines.

The classical analytical method for expansive pressure estimation in a thick-walled cylinder has been used extensively in previous research, however, it has never been validated with direct measurement of the actual internal pressure in the cylinder. A series of tests employing direct pressure measurement using high-capacity pressure sensor was carried out. The results show that the actual expansive peak pressure is consistently higher than the estimated peak pressure from the analytical model. A correction factor α=1.31 is derived with R^2=0.999. Finally, a new methodology based on iterative procedure is developed using axisymmetric finite element modelling and test results to derive the SCDA modulus of elasticity. Recognizing the variation of pressure and elasticity with time, the focus is on the peak pressure and hence the peak modulus of elasticity. The methodology reveals that the modulus of elasticity of expansive cement at peak pressure is on average 8.2 GPa with a coefficient of variation of only 0.012. This result should prove useful in numerical modelling studies of SCDA hole pattern design in practical mining applications.

Acknowledgements

This work was financially supported by a research grant from Natural Resources Canada, Clean Growth Program (No. CGP-17-1003) and industry partner Newmont Corporation. The authors are grateful for their support.

References

[1] Soeda K, Harada T. The mechanics of expansive pressure generation using expansive demolition agent. Doboku Gakkai Ronbunshu 1993;1993(466):89–96.
[2] Bentur A, Ish-Shalom M. Properties of type K expensive cement of pure components II. Proposed mechanism of ettringite formation and expansion in unrestrained paste of pure expansive component. Cem Concr Res 1974;4(5):709–21.
[3] De Silva RV, Gamage RP, Anne Perera MS. An alternative to conventional rock fragmentation methods using SCDA: a review. Energies 2016;9:1–31.
[4] Harada T, Idemitsu T, Watanabe A, Takayama SI. The design method for the demolition of concrete with expansive demolition agents. Fract Concr Rock 1989.
[5] Laefer DF, Ambrozevitch-Cooper N, Huynh MP, Midgette J, Ceribasi S, Wortman J. Expansive fracture agent behaviour for concrete cracking. Mag Concr Res 2010;62(6):443–52.
[6] Hanif M. Effective use of expansive cement for the deformation and fracturing of granite. Gazi Univ J Sci 2010;20:1–5.
[7] Natanzi AS, Laefer DF, Connolly L. Cold and moderate ambient temperatures effects on expansive pressure development in soundless chemical demolition agents. Constr Build Mater 2016;110:117–27.
[8] Hinze J, Brown J. Properties of soundless chemical demolition agents. Constr Eng Manag 1995;120(4):816–27.
[9] Hanif M. Deformation behaviour of rock around a borehole filled with an expansive cement. J King Abdulaziz Univ Sci 1997;9(1):93–107.
[10] Cohen MD. Modeling of expansive cements. Cem Concr Res 1983;13(4):519–28.
[11] Kim K, Cho H, Sohn D, Koo J, Lee J. Prediction of the minimum required pressure of soundless chemical demolition agents for plain concrete demolition. J Comput Struct Eng. Inst. Korea 2018;31(5):251–328.
[12] Shang J, Hencher SR, West LJ, Handley K. Forensic excavation of rock masses: a technique to investigate discontinuity persistence. Rock Mech Rock Eng 2017;50(11):2911–28.
[13] Parker PN. Expanding cement - a new development in well cementing. J Petroleum Technol 1966;18(5):559–64.

[14] De Silva VRS, Ranjith PG, Perera MSA, Wu B, Rathnaweera TD. A modified, hydrophobic soundless cracking demolition agent for non-explosive demolition and fracturing applications. Process Saf. Environ. Prot 2018;119:1–13.
[15] Wang LC, Duan K, Zhang QY, Li XJ, Jiang RH. Study of the dynamic fracturing process and stress shadowing effect in granite sample with two holes based on SCDA fracturing method. Rock Mech Rock Eng 2022;55(3):1537–53.
[16] Arshadnejad S, Goshtasbi K, Aghazadeh J. A model to determine hole spacing in the rock fracture process by non-explosive expansion material. Int J Miner Metall Mater 2011;18(5):509–14.
[17] Tang W, Zhai C, Xu JZ, Sun Y, Cong YZ, Zheng YF. The influence of borehole arrangement of soundless cracking demolition agents (SCDAs) on weakening the hard rock. Int J Min Sci Technol 2021;31(2):197–207.
[18] Zhang Q, He MC, Wang J, Guo S, Guo ZB, Liu XY, Hu JZ, Ma ZM, Fan LX, Guo PF. Instantaneous expansion with a single fracture: a new directional rock-breaking technology for roof cutting. Int J Rock Mech. Min. Sci 2020:132 104399.
[19] Xu S, Hou PY, Li RR, Cai M. An experimental study on the mechanical properties and expansion characteristics of a novel self-swelling cartridge for rock breakage. Rock Mech Rock Eng 2021;54:819–32.
[20] Betonamit. n.d. Available from: https://www.betonamit.com/en/ 2021 (Accessed 17 September 2021).
[21] Bristar cracking agent and expansive mortar. n.d. Available from: https://www.silentech.com.au/bristar.html (Accessed 17 September 2021).
[22] Dexpan. n.d. Dexpan. Available from: https://www.dexpan.com/ (2021) (Accessed 17 September 2021).
[23] Expando. Available from: https://expando.com.au/ 2021 (Accessed 17 September 2021).
[24] Ecobust. Available from: http://www.ecobust.com/ 2011 (Accessed 17 September 2021).
[25] Timoshenko JS, Goodier. Theory of elasticity. Phys Contin Media 1951:234–59.
[26] Laefer DF, Natanzi AS, Zolanvari SMI. Impact of thermal transfer on hydration heat of a soundless chemical demolition agent. Constr Build Mater 2018;187:348–59.
[27] Soeda KH. Fast-acting non-explosive demolition agent. Con Demolition Reuse Concr 1994:231–41.
[28] Gholinejad M, Arshadnejad S. An experimental approach to determine the hole-pressure under expansion load. J. South. African Inst Min Metall 2012;112(7):631–65.
[29] Dowding CH, Labuz F. Fracturing of rock with expansive cement. J Geotech Eng Div 1982;108(10).
[30] Xu S, Hou PY, Li RR, Suorineni FT. An improved outer pipe method for expansive pressure measurement of static cracking agents. Int J Min Sci Technol 2022;32(1):27–39.
[31] Hoek E, Martin CD. Fracture initiation and propagation in intact rock: a review. J Rock Mech Geotech Eng 2014;6(4):287–300.
[32] Peng J, Rong G, Cai M, Wang XJ, Zhou CB. An empirical failure criterion for intact rocks. Rock Mech Rock Eng 2014;47(2):347–56.
[33] Park J, Kim K. Use of drilling performance to improve rock-breakage efficiencies: a part of mine-to-mill optimization studies in a hard-rock mine. Int J Min Sci Technol 2020;30(2):179–88.